CALORIMETRY, EXCESS HEAT, AND FARADAY EFFICIENCY IN Ni-H_2O ELECTROLYTIC CELLS

ELECTROLYTIC DEVICES

KEYWORDS: *calorimetry, Faraday efficiency, excess heat*

ZVI SHKEDI, ROBERT C. McDONALD, JOHN J. BREEN, STEPHEN J. MAGUIRE, and JOE VERANTH
Bose® Corporation, Framingham, Massachusetts 01701

Received May 31, 1994
Accepted for Publication August 1, 1994

Apparent excess heat is observed in light water electrolytic cells containing a variety of nickel cathodes, a platinum anode, and an electrolyte of K_2CO_3 in H_2O. High-accuracy calorimetric measurements show apparent excess heat in the range of 15 to 37% of input power if a 100% Faraday efficiency is assumed for H_2 and O_2 gas release. The H_2 and O_2 gases released during electrolysis are recombined in a vessel external to the cell, and the quantity of recombined H_2O is compared with the quantity of H_2O expected from 100% efficient electrolysis. The measured Faraday efficiency is shown to be significantly <100%, and conventional chemistry can account for the entire amount of observed apparent excess heat to within an accuracy of better than 0.5%.

I. INTRODUCTION

Several recent publications reported the observation of excess heat upon electrolysis of an aqueous alkali-carbonate electrolyte using a variety of metallic cathodes. Mills and Kneizys[1] reported excess heat in the range of 150 to 3700% using a nickel cathode and pulsed electrolysis. Noninski,[2] Bush,[3] Notoya,[4] Srinivasan et al.,[5] and others also reported the observation of excess heat in a variety of alkali-carbonate electrolytes. To explain the source of the observed excess heat, Mills and Kneizys presented a theory whereby hydrogen atoms undergo transitions to quantized energy levels lower than the conventional ground state to form hydrino atoms. Bush rejected the novel theory presented by Mills and Kneizys in favor of an alkali-hydrogen cold fusion reaction theory.

Since the original publication by Fleischmann and Pons[6] announcing the discovery of excess heat in Pd-D_2O electrochemical cells, questions have been asked regarding the application of rigorous experimental methodology in accounting for all the energy invested in and flowing out of such cells. One area of concern has been the common assumption that the Faraday efficiency for evolution of H_2 (or D_2) and O_2 gas is 100%. Another area of uncertainty has been the accuracy of calorimetric measurements.

Noninski offers a discussion of the Faraday efficiency along with the possibility of competing electrochemical reactions in the electrolyte and the possibility of internal recombination of H_2 and O_2 and concludes that further experimental investigation is necessary. A detailed investigation of the Faraday efficiency in light water cells is presented here along with a sensitive and accurate measurement technique.

In the area of calorimetry, Fleischmann and Pons[6,7] report measurements using a heat-loss type calorimeter. A similar approach using a closed cell with an internal recombiner is described by Eagleton and Bush.[8] McKubre et al.[9] and Storms[10] also describe calorimetric measurements in closed cells using a flow calorimeter. A significant improvement in the accuracy of calorimetric measurements using a new design of a heat-loss type calorimeter is presented here with a clear demonstration of improved absolute accuracy and long-term stability.

All reports of observed excess heat in an open electrolytic cell involve a correction for the enthalpy of formation (ΔH) of liquid H_2O to form H_2 and O_2 gas. This correction, equal to $\Delta H = 285.8$ kJ/mol (Ref. 11), has been generally applied as a subtraction of 1.481 V from the cell voltage (V). The net result of such a correction was that the thermal energy input to the cell was assumed by all investigators to be

$$E_{in} = \int (V - 1.481) I \, dt \ , \qquad (1)$$

where I is the cell current. The validity of Eq. (1) warrants further investigation in view of the lack of sufficient experimental evidence that the Faraday efficiency of H_2 and O_2 gas evolution is indeed 100%.

In closed cells with an internal recombiner, the unknown contributions of competing reactions and internal recombination are avoided. Since the evolving H_2 and O_2 gases are internally recombined, 1.481 V is not subtracted from the cell voltage, so this element of uncertainty in the thermal energy input to the cell is removed. However, a fraction of the heat is dissipated by the recombiner in the air space above the electrolyte, thus changing the spatial distribution of heat flow from the cell. This is a possible source of calibration errors. One method to improve the calibration accuracy is to use an inert cathode (e.g., platinum) or to use reverse electrolysis as performed by Eagleton and Bush.[8] However, until it is conclusively shown that the Faraday efficiency does not vary between calibration and operation of the cell and does not vary with hydrogen loading of the cathode during normal operation, claims of excess heat in closed cells may still be subject to calibration errors.

A significant improvement in calibration and in the accuracy of determining energy input to the cell can be realized by recombining the evolving H_2 and O_2 gases in a recombination vessel external to the cell and calorimeter. By comparing the quantity of recombined H_2O to the quantity of H_2O expected from 100% efficient electrolysis, one can determine the actual Faraday efficiency and accurately account for all the energy invested in the cell.

II. DETERMINATION OF FARADAY EFFICIENCY AND CELL ENERGY BALANCE

In an aqueous electrolytic cell, the cell current has three components:

1. I_e, which is the electrolysis current evolving H_2 and O_2 gas that leaves the cell
2. I_{er}, which is the electrolysis current evolving H_2 and O_2 gas that recombines inside the cell
3. I_p, which is the parasitic current that does not evolve H_2 or O_2 gas.

The total cell current is the sum of the three components:

$$I = I_e + I_{er} + I_p \ . \tag{2}$$

The thermal power input to the cell is given by

$$P_{in} = (I_{er} + I_p)V + I_e(V - 1.481) = VI - 1.481 I_e \ , \tag{3}$$

where V is the anode-to-cathode cell voltage. The subtraction of 1.481 V may be applied only to the I_e component of the cell current since the I_{er} and I_p components do not release H_2 and O_2 gas that leaves the cell.

The relative magnitudes of I_e, I_{er}, and I_p can vary, in general, as a function of cell voltage, electrode materials, loading ratio of hydrogen or deuterium in the cathode, electrode surface areas, contaminants in the electrolyte, and electrode current densities. In pulsed-current experiments, I_e, I_{er}, and I_p can also vary with frequency and duty cycle. Pulsed-current electrolysis presents a further complication as the cell voltage and current are not necessarily in phase and may vary with time within the pulse of applied current.

If the duty cycle of the current pulses is low, I_{er} can become a dominant fraction of the total cell current since internal H_2-O_2 recombination takes place 100% of the time while the electrical power input is integrated over only a small fraction of time equal to the duty cycle of the pulses.

By recombining the escaping H_2 and O_2 gases using a high-efficiency recombiner in a separate vessel outside the cell to form H_2O, we can determine the I_e component of the cell current using Faraday's law:

$$2FM/18.015 = \eta \int I_e \, dt \ , \tag{4}$$

where

M = mass of the externally recombined H_2O (g)

F = Faraday constant

η = recombiner efficiency.

Once we measure M and η, we can also determine the Faraday efficiency of H_2 and O_2 gas release, which is given by

$$\textit{Faraday efficiency} = \frac{2FM}{18.015\eta \int I \, dt} \ . \tag{5}$$

Determining the relative magnitudes of I_{er} and I_p is more difficult. However, for the purpose of calculating cell energy balance or for determining the Faraday efficiency of H_2 and O_2 gas release, separation of I_{er} and I_p is not necessary.

Using Eq. (3), we find that the integrated thermal energy input to the cell in joules is

$$E_{in} = \int P_{in} \, dt = \int VI \, dt - 1.481 \int I_e \, dt \ . \tag{6}$$

Combining Eqs. (4) and (6) yields the desired expression for the total cell energy input:

$$E_{in} = \int VI \, dt - 15\,864 \, M/\eta \ . \tag{7}$$

It follows that for proper determination of cell energy input, measurement of only the electrical energy

$\int VI\,dt$ is not sufficient. One must also measure M and η.

Any excess heat is given by

$$E_{ex} = E_{out} - E_{in} = E_{out} - \int VI\,dt + 15\,864\,M/\eta \ , \tag{8}$$

where E_{out} is the total thermal energy developed in the cell.

III. CELL CONSTRUCTION

Each experiment consisted of an electrolytic cell inside a calorimeter, an H_2-O_2 recombination vessel, and a gas monitor. The cell, the recombination vessel, and the gas monitor were connected with Tygon® tubes, as shown in Fig. 1.

The electrolytic cell consisted of a borosilicate glass beaker filled with 90 ml of 0.57 M K_2CO_3 in high-performance liquid chromatography-grade H_2O, a nickel cathode, a platinum anode, a nickel-chromium resistive heater for calibration, and a thermistor inside a bottom-sealed polytetrafluoroethylene (PTFE) tube. All electrical lead wires were covered with PTFE tubes, and the only materials in contact with the electrolyte were glass, nickel, platinum, and PTFE. A schematic view of the cell is shown in Fig. 2.

Two types of cathodes were used. Type A cathodes were made of 10 000 turns of cold drawn nickel wire, 99.95% pure, 25 μm in diameter (Molecu, New Jersey), wound in a loose coil around a mandrel of 9.7-mm-diam cylindrical nickel tube with perforated walls. Total wire length was ~425 m. The coil winding pattern was designed to give a volume fill factor of ~3% nickel, allowing 97% of the space within the coil volume to be filled with the electrolyte. The nickel coil assembly was cleaned by soaking it in acetone and methanol and was sintered at 1100°C for 2 h in an atmosphere of 95% argon/5% H_2 at atmospheric pressure. Type B cathodes were made of Fibrex® sintered nickel mesh (National Standard, 80% fiber/20% powder) rolled in two layers around the same nickel mandrel as in type A cathodes and secured with two turns of 1-mm nickel wire. Type B cathodes were not cleaned or sintered after assembly. Electrical connection to the cathode was provided by tack welding a 0.5-mm platinum wire to the nickel mandrel.

The anode was made of a spiral of 99.99% pure platinum wire, 121 cm long and 0.5 mm in diameter. The anode spiral diameter was ~2.5 cm.

The resistive heater was made of Ni-Cr wire soldered to copper lead wires. The entire length of the Ni-Cr resistive element was immersed under the electrolyte level near the bottom of the cell to ensure that all of the thermal energy developed in the resistive element would be dissipated in the electrolyte and not in the air space above it. The Cu/Ni-Cr/Cu assembly was snaked through a thin PTFE tube, and both ends of the PTFE tube came out of the cell through the cell cover. This configuration prevented any contact between the electrolyte and the heater materials.

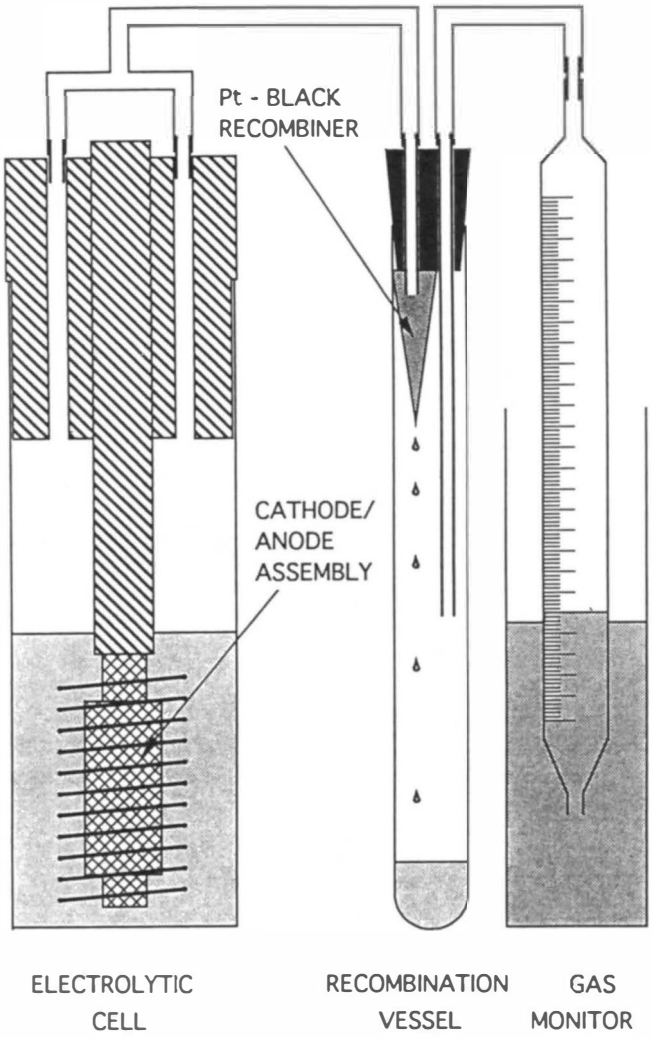

Fig. 1. The H_2 and O_2 gases from the cell flow to the recombination vessel and recombine on the platinum-black recombiner. Recombined H_2O accumulates at the bottom of the vessel. Residual H_2 and O_2 gases that do not recombine flow to the gas monitor and displace an equivalent volume of oil in the graduated monitor tube.

Each cell had a thermistor inside an oil-filled bottom-sealed PTFE tube placed at the center of the nickel mandrel to monitor the electrolyte temperature. However, the electrolyte temperature was not used for calorimetry, as is shown in Sec. IV.

The cathode, the anode, the heater, and the thermistor tube were mounted to a PTFE cover that was sealed to the glass beaker with a rubber O-ring. All

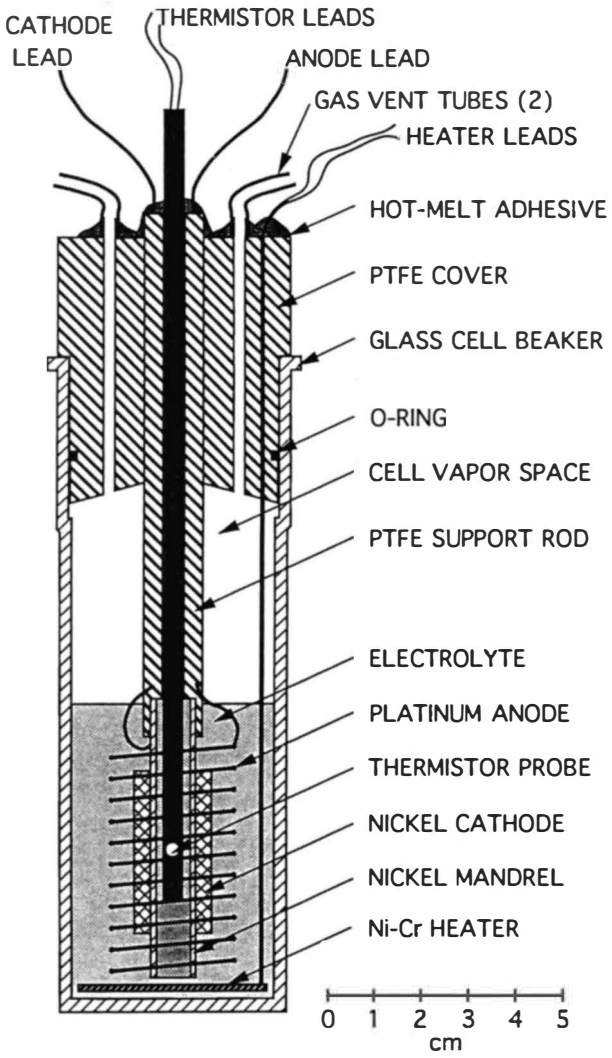

Fig. 2. Detailed view of the electrolytic cell.

feed-through connections and mountings were hermetically sealed to the cover using hot-melt glue. Two openings in the cover were fitted with polypropylene tube connectors. Tygon® tubes connected these openings to the recombination vessel. Even though one such opening was sufficient from the functional point of view, it has been recommended[12] that all such cells be fitted with redundant openings to avoid accidental pressure buildup in the cells in case one opening becomes plugged. The availability of redundant openings in the cell cover also made it easy to refill the cell with H_2O to replenish the quantity of H_2O that left the cell through electrolysis.

The recombination vessel was a 25-ml test tube with a two-hole rubber stopper. Stainless steel tubes inserted into the stopper holes served as fittings for connecting the Tygon® tubes. A 1-cm^2 catalytic recombiner, made in-house with platinum-black on porous PTFE, was clamped between the stopper and the wall of the test tube. As the H_2 and O_2 gases recombined on the recombiner, the H_2O vapor condensed and accumulated in the test tube.

The gas monitor (shown in Fig. 1) was connected to the recombination vessel to monitor the recombiner efficiency. A 25-ml graduated pipette was partially filled with low-vapor-pressure oil. The bottom of the pipette was dipped in an oil container while the top of the pipette was connected to the recombination vessel. The oil container could be moved up and down to adjust the oil level in the container to be equal to the oil level inside the pipette, thus eliminating gas volume variations due to hydrostatic pressure buildup. Any H_2-O_2 recombination inefficiencies in the recombiner would show up as a displacement of an equivalent volume of oil inside the pipette due to the escaping H_2 and O_2 gases.

To ensure personnel safety, we designed and constructed the experimental setup with a high likelihood of an explosion in mind. The platinum-black recombiner is capable of igniting the H_2-O_2 gas mixture thereby causing an explosion. Several cells have been destroyed through such explosions. All explosions happened while connecting or disconnecting tubes between the cell, the recombination vessel, and the gas monitor or when trying to remove the accumulated water from the recombination vessel. Each explosion is believed to have been triggered by a sudden increase in the flow rate of the H_2-O_2 gas mixture in the recombination vessel. The explosion may have started inside the recombination vessel, propagated through the interconnecting tubes, and ignited the H_2-O_2 gas mixture in the cell. Any operation that might restrict the free flow of gas from the cell or any operation that may cause a sudden increase in the flow rate of H_2 or O_2 toward the recombiner should be avoided. For additional safety recommendations, see Ref. 13.

IV. CALORIMETRY

The calorimeters were carefully designed to overcome some critical weaknesses that have been noticed in publications claiming the observation of excess heat:

1. Unaccounted thermal losses, especially through the cell cover, were reduced to a level comparable to the measurement error of the calorimeter.

2. In closed cells that include an internal recombiner, calibration must be performed with an equal rate of heat generation in the actual location of the recombiner, as heat generated in the recombiner near the top of the cell changes the spatial distribution of heat flow from the cell. Such cells were calibrated with actual electrolysis current using an inert cathode.

3. Open cells cannot be properly calibrated with electrolysis current unless the Faraday efficiency is precisely known. To avoid any errors due to unknown

and possibly unstable Faraday efficiency, a calibration heater was used. It was fully immersed in the electrolyte, in close proximity to the location of heat generation in the actual cells. The difference in the heat-flow distribution due to the lack of bubbles during calibration was found to be insignificant. This was one of the benefits of the low level of unaccounted thermal losses from the calorimeter.

4. Variations in electrolyte level during operation of the cell (due to electrolysis of H_2O) were initially found to have a measurable effect on the calorimeter calibration coefficients since the spatial distribution of thermal resistance for heat loss from the cell varies with electrolyte level. To overcome this sensitivity, we fine tuned the geometry of the calorimeters and the location of the temperature probes until the calorimeter calibration coefficients were insensitive to variations in electrolyte level near the desired operating point.

5. Using the temperature difference between the cell electrolyte and the ambient surrounding the calorimeter (usually water) was found to be the most significant source of error. This error is equivalent to the error in trying to measure the electrical resistance of a low-value resistor using high current and a two-wire measurement. The accuracy of a four-wire measurement of electrical resistance is far superior to that of a two-wire measurement. The same holds true for calorimetry. The calorimeters were designed therefore to employ the equivalent of a four-wire measurement in which the temperature drop caused by the heat flux from the cell was measured across a stable thermal resistor with equithermal terminations. The temperatures of the heat source (the cell) and the heat sink (the cooling water) were not considered for calorimetry.

Eight calorimeters were designed and fabricated at the Bose engineering laboratories. The calorimeters were of the heat loss type and consisted primarily of two concentric copper cups with a silicone rubber thermal insulation layer between the cups. A schematic view of a calorimeter is shown in Fig. 3.

The outer copper cup was maintained at a constant temperature of 30.0°C with temperature-controlled circulating water. The electrolytic cell was placed inside the inner copper cup. The gap between the glass beaker and the inner copper cup was filled with low-vapor-pressure oil for thermal contact. The overall thermal resistance from the cell electrolyte to the inner copper cup and from the inner copper cup to the outer copper cup was ~1.5 and 0.95°C/W, respectively.

Thermal energy developed in the cell flows out through the inner copper cup, the silicone rubber, and the outer copper cup. The average temperature difference between the copper cups is a very precise measure (after calibration) of the heat flux flowing out of the cell. A small fraction of the thermal energy (~10 to 20 mW) is lost through the top of the cell and is not integrated by the copper cups. However, since exactly the same fraction is lost during calibration, the net result is no loss of accuracy.

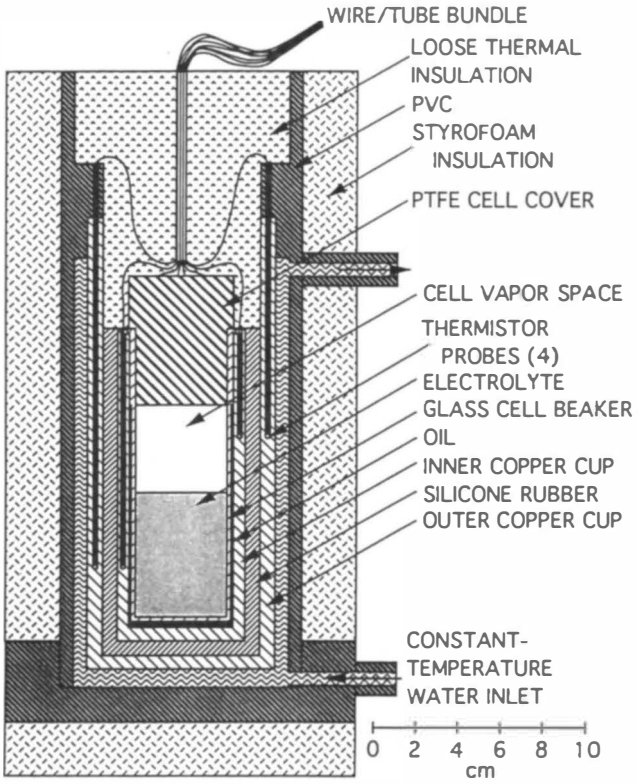

Fig. 3. Cross section through a calorimeter. The internal details of the electrolytic cell (see Fig. 2) have been omitted for clarity.

The space above the cell cover was filled with crumpled paper towels and foam insulation sheets for thermal insulation. The thermal resistance for heat loss from the cell to the outside world through the cover and the top insulation was ~650°C/W. This path for heat loss reflects itself in the value of the coefficient A_0 in Eq. (9).

The temperature of each of the copper cups was monitored with two 10-kΩ (at 25°C) glass-sealed thermistors inserted into vertical holes that were drilled in the walls of the copper cups and filled with oil. A fifth thermistor, protected with a bottom-sealed and oil-filled PTFE tube, was inserted into the cell electrolyte for monitoring the electrolyte temperature. All thermistors were aged for many weeks at high temperature to reduce long-term drift and were calibrated against a National Institute of Standards and Technology traceable standard to an absolute accuracy of ±0.1°C and a relative (or differential) accuracy of ±0.004°C.

Cell electrolysis current and cell heater current were determined by measuring the voltage across wire-wound 0.5-Ω current-sense resistors that were heat sunk

to a large aluminum plate and calibrated using a high-accuracy current source.

The data acquisition system consisted of a multiplexed, 16-bit, variable gain, analog-to-digital converter and a MacII computer. All the electrical wiring connecting the data acquisition system with the cells and calorimeters consisted of twisted and shielded pairs. All electrical sense lines were separated from current-carrying lines. All electrical parameters (electrolysis and heater voltage, electrolysis and heater current, and thermistor resistance) were measured once per second, averaged over a 2-min period, and recorded once every 2 min.

For calibration, the calorimeters and cells were fully assembled as described earlier, and the heater power was stepped every 6 h for several days until the entire power range of interest was covered. The nickel cathode was maintained at a cathodic voltage of ~0.7 V and a cell current of ~0.1 mA during calibration.

The calorimeter response was fitted to a third-order polynomial:

$$\textit{heater power} = dE_{out}/dt = \sum_{i=0}^{3} A_i(\Delta T)^i \ , \qquad (9)$$

where A_i are calibration coefficients and ΔT is the averaged temperature difference between the inner copper cup and the outer copper cup at steady state.

A typical calibration curve of a calorimeter and the values of the calibration coefficients (A_i) are shown in Fig. 4. The circles in each graph represent actual data points while the solid line represents the best fit. The averaged temperature difference between the inner and outer copper cups is shown in Fig. 4a as a function of input power. The deviations of individual calibration points from the best-fit line are shown in Fig. 4b with a root-mean-square (rms) value of 0.00063 W corresponding to 0.016% of full scale.

A long-term zero-balance response of a calibrated calorimeter is shown in Fig. 5. Interestingly, the calorimeter shown in Fig. 5 was a closed cell with a palladium cathode in a 0.1 *M* LiOD electrolyte. This calorimeter was operated for 256 days with no traces of excess heat nor loss of accuracy. Each data point in Fig. 5 represents excess energy as a fraction of the total input energy to the cell, both integrated over a 48-h period. Significant deviations from the zero line occurred only upon changes in the input power to the cell or upon power failures that stopped the flow of the constant-temperature cooling water. Cell current was not interrupted during power failures. No long-term drift was noticeable during the entire operating period. The absolute accuracy of the calorimeter can be appreciated from $E_{ex}/E_{in} = 2.4 \times 10^{-4}$, which represents the overall ratio of excess energy relative to input energy, both integrated over the entire range of day 10 to day 256. This level of accuracy is equivalent to an average power accuracy of 0.6 mW.

V. EXPERIMENTAL PROCEDURE

Four cells were operated simultaneously at direct-current cell currents of 0.18, 0.35, and 0.6 A. After startup of each cell and after a change in the cell current, the calorimeters were allowed to reach thermal steady state (4 to 6 h). Data recorded during this stabilization period were ignored. For each of the cells, the integrated electrical energy input ($\int VI\,dt$), the cell thermal energy output (E_{out}), and the weight of the H_2O accumulated in the recombination vessel were recorded simultaneously at irregular intervals ranging from 4 h to 4 days.

To test for the possibility of H_2O evaporation from the cell and condensation in the recombination vessel, we removed the recombiner from the recombination vessel for several days. The recombination vessel remained completely dry with no traces of condensation.

To determine the recombiner efficiency, we assumed the volume of oil displaced in the gas monitor to be equal to the volume of H_2 and O_2 gas that escaped the recombiner. All the H_2 and O_2 gases that left the cell were either collected as H_2O in the recombination vessel or as gas in the gas monitor. Using Faraday's law, we determined that 0.6 ± 0.2% of the H_2 and O_2 gases that left the cell failed to recombine in the recombination vessel. Hence, the recombiner efficiency was established as $\eta = 0.994$.

Approximately every 2 to 4 days, the H_2O accumulated in the recombination vessel was returned to the cell to maintain a constant volume of electrolyte.

After a number of measurement cycles, two of the cells (W12E6 and W16E7) were intentionally contaminated by adding 25 mg of $CuSO_4$, 8 mg of Fe_2O_3 dissolved in HCl, and 100 mg of "Micro" liquid detergent to the electrolyte. The purpose of the intentional contamination was to study its effect on the Faraday efficiency. The addition of copper was suggested by Bush.[14]

VI. RESULTS

Tables I through IV show the operating conditions and the measurement results for each of the four cells. Each line in Tables I through IV represents an experiment interval that lasted for a number of days, as shown in the "duration" column. The first two columns show the cell current (I) and the presence of additives, if any, in each of the experiments. The column labeled "$\int VI\,dt$" shows the total integrated electrical energy input, "E_{out}" is the thermal energy output as determined by the calorimeter, and "M" is the quantity of H_2O accumulated in the recombination vessel. The actual energy input to the cell in each experiment interval (E_{in}) was calculated using Eq. (7), and the Faraday efficiency was calculated using Eq. (5).

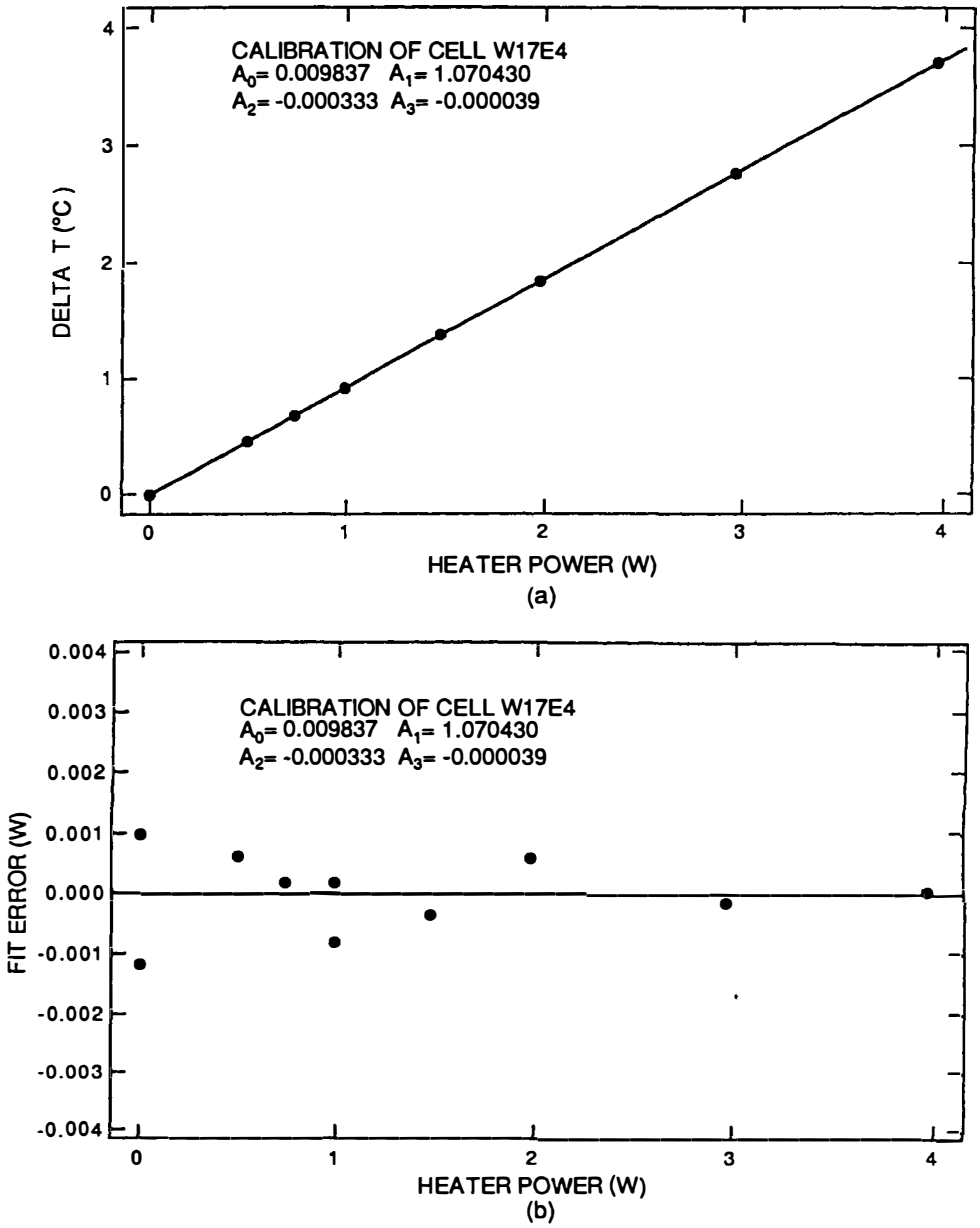

Fig. 4. (a) A typical calibration curve of a calorimeter and the calibration coefficients (A_i) and (b) the deviations of individual calibration points from the best-fit line.

Two approaches were taken to determine excess heat. The conventional approach assumes that the Faraday efficiency is 100%. In that case, the apparent excess heat is given by

$$\textit{apparent excess heat}\ (\%) = 100 \cdot \frac{E_{out} - \int (V - 1.481) I\, dt}{\int (V - 1.481) I\, dt} \,. \qquad (10)$$

On the other hand, if the actual Faraday efficiency is taken into account, then the real excess heat (E_{ex}) is calculated using Eq. (8). The last two columns in Tables I through IV show the apparent excess heat and the percentage ratio of real excess heat ($100 \cdot E_{ex}/E_{in}$) for each of the experiments.

The overall weighted average of E_{ex}/E_{in} for each of the cells is shown in Table V along with the grand total of E_{ex}/E_{in} for all four cells combined. The grand total of $E_{ex}/E_{in} = 0.13 \pm 0.48\%$ clearly indicates that there is no real excess heat in these Ni-K_2CO_3-H_2O electrolytic cells.

The additions of $CuSO_4$, Fe_2O_3, or Micro detergent to cells W12E6 (Table I) and W16E7 (Table III) did not have a notable influence on the Faraday efficiency or

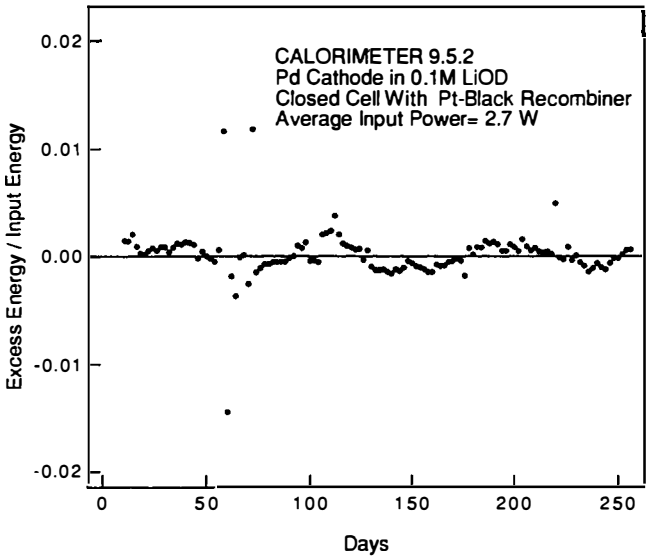

Fig. 5. A long-term zero-balance response of a calibrated calorimeter.

on the apparent excess heat. This result suggests the need for further investigation in view of somewhat contrasting observations by Srinivasan et al.,[15] who report an increase in the apparent excess heat in the presence of copper metal and a decrease or total disappearance of apparent excess heat in the presence of stainless steel.

Changing the cell current had a more observable effect. In the noncontaminated cells W15E5 (Table II) and W17E4 (Table IV), the current was first reduced from 0.35 to 0.18 A, then it was increased to 0.6 A. Reducing the current caused a small decrease in the Faraday efficiency and an increase in the apparent excess heat of cell W17E4. This effect was reversed upon increasing the current to 0.6 A. In cell W15E5, reducing the current had no significant effect; however, raising the current to 0.6 A increased the Faraday efficiency to near 100% while reducing the apparent excess heat to near zero.

In all the cells and all the experiments, the real excess heat hovered at about zero with a weighted rms deviation of ~1% and was not affected by any of the cell operating conditions.

To conclude the experiments, we relocated two of the recombiners from the recombination vessels to inside the cells to form closed-cell experiments. Each recombiner was suspended from the PTFE cell cover, hanging vertically in the vapor space above the electrolyte. No other changes were made to the cell/recombination-vessel/gas-monitor system. In this closed-cell configuration, all the electrical energy was invested in the cell, and no correction was applied for the enthalpy of formation of H_2 and O_2 gas from liquid H_2O.

TABLE I

Operating and Performance Parameters of Cell W12E6
Cathode Type A (Nickel Coil)

Cell Current (A)	Additives[a]	Duration, t (days)	$\int VI\,dt$ (J)	E_{out} (J)	M H_2O (g)	E_{in} (J)	Faraday Efficiency (%)	Apparent Excess Heat (%)	E_{ex}/E_{in} (%)
0.350	---	1.1245	96 350	57 659	2.38	58 365	75.42	25.38	−1.21
0.350	---	2.8845	255 289	153 187	5.91	160 966	73.01	21.48	−4.83
0.350	---	0.9867	86 995	52 104	2.15	52 681	77.65	21.73	−1.10
0.350	---	1.0412	91 574	54 678	2.32	54 547	79.40	21.67	0.24
0.350	---	0.1970	17 350	10 151	0.45	10 168	81.39	19.06	−0.17
0.350	---	0.7304	64 255	37 999	1.62	38 400	79.04	20.46	−1.04
0.350	---	1.0504	92 369	54 415	2.40	54 065	81.42	20.05	0.65
0.350	---	3.0014	269 841	159 095	7.00	158 122	83.11	17.48	0.61
0.350	---	0.9837	90 327	53 103	2.32	53 300	84.04	14.77	−0.37
0.350	---	0.2978	27 212	15 962	0.71	15 880	84.96	15.04	0.51
0.350	Cu	0.7111	67 398	39 957	1.72	39 947	86.19	12.40	0.02
0.350	Cu	1.2000	113 539	68 691	2.83	68 372	84.04	14.88	0.47
0.350	Cu	0.7926	74 663	45 257	1.85	45 137	83.18	15.55	0.26
0.350	Cu, Fe	3.9939	368 730	226 296	8.48	233 391	75.66	19.19	−3.04
0.350	Cu, Fe	0.9837	91 121	55 731	2.19	56 169	79.33	18.42	−0.78
0.600	Cu, Fe	0.9171	154 665	99 499	3.51	98 646	79.56	18.09	0.86
0.600	Cu, Fe	0.7941	134 717	86 939	2.95	87 635	77.22	17.88	−0.80

[a]"Cu" indicates 25 mg of $CuSO_4$, "Fe" indicates 8 mg of Fe_2O_3 predissolved in 1 ml of HCl.

TABLE II

Operating and Performance Parameters of Cell W15E5
Cathode Type A (Nickel Coil)

Cell Current (A)	Additives[a]	Duration, t (days)	$\int VI\,dt$ (J)	E_{out} (J)	M H_2O (g)	E_{in} (J)	Faraday Efficiency (%)	Apparent Excess Heat (%)	E_{ex}/E_{in} (%)
0.350	---	0.7231	64621	36547	1.67	37968	82.30	13.37	−3.74
0.350	---	2.8933	256600	148829	6.58	51584	81.04	17.17	−1.82
0.350	---	0.9823	86075	49966	2.14	51921	77.64	18.73	−3.77
0.350	---	1.0487	90816	52245	2.36	53150	80.20	19.14	−1.70
0.350	---	0.1911	16482	9446	0.43	9619	80.18	19.22	−1.80
0.350	---	0.7319	62762	35788	1.65	36428	80.34	19.35	−1.76
0.350	---	1.0504	89131	50193	2.41	50667	81.76	19.26	−0.94
0.350	---	3.0028	253888	143491	6.75	46159	80.11	20.17	−1.83
0.350	---	0.9823	83667	48883	2.11	49991	76.55	23.20	−2.22
0.350	---	1.0089	85319	48760	2.26	49249	79.82	21.49	−0.99
0.350	---	1.2000	102324	58224	2.72	58913	80.77	19.85	−1.17
0.180	---	0.7867	32625	18390	0.87	18740	76.63	26.78	−1.87
0.180	---	4.0458	167692	90365	4.65	93479	79.64	21.28	−3.33
0.180	---	0.9808	41726	21469	1.22	22255	86.19	12.19	−3.53
0.600	---	0.9126	149119	82651	4.29	80651	97.72	4.55	2.48
0.600	---	0.7956	132196	71301	3.77	72027	98.50	0.26	−1.01

[a]This cell had no additives.

TABLE III

Operating and Performance Parameters of Cell W16E7
Cathode Type B (Nickel Fibrex)

Cell Current (A)	Additives[a]	Duration, t (days)	$\int VI\,dt$ (J)	E_{out} (J)	M H_2O (g)	E_{in} (J)	Faraday Efficiency (%)	Apparent Excess Heat (%)	E_{ex}/E_{in} (%)
0.350	---	2.8149	248975	150912	6.07	152099	76.84	22.78	−0.78
0.350	---	1.0030	89108	55298	2.04	56550	72.48	25.14	−2.21
0.350	---	1.0324	91480	56826	2.17	56847	74.91	25.60	−0.04
0.350	---	0.2044	18129	11299	0.43	11266	74.95	25.92	0.29
0.350	---	0.7304	64693	40470	1.51	40593	73.67	26.54	−0.30
0.350	---	1.0489	92691	57851	2.20	57579	74.74	26.55	0.47
0.350	---	3.0014	267504	169578	6.22	168234	73.85	27.42	0.80
0.350	---	0.9837	88821	57675	1.94	57859	70.28	28.84	−0.32
0.350	---	0.2978	26790	17066	0.62	16894	74.19	26.85	1.01
0.350	Cu	0.7126	65545	42122	1.48	41924	74.01	25.25	0.47
0.350	Cu	1.1986	110564	71278	2.50	70664	74.33	25.30	0.87
0.350	Cu, Det	0.7941	74092	48482	1.63	48077	73.15	25.84	0.84
0.350	Cu, Det	4.0324	377694	240037	8.76	237886	77.42	21.78	0.90
0.350	Cu, Det	0.9867	93056	57093	2.26	56986	81.62	16.84	0.19
0.600	Cu, Det	0.9200	157829	101039	3.62	100054	81.79	15.88	0.98
0.600	Cu, Det	0.7956	135874	86067	3.18	85121	83.09	15.07	1.11

[a]"Cu" indicates 25 mg of $CuSO_4$; "Det" indicates 100 mg of Micro detergent.

TABLE IV

Operating and Performance Parameters of Cell W17E4
Cathode Type B (Nickel Fibrex)

Cell Current (A)	Additives[a]	Duration, t (days)	$\int VI\,dt$ (J)	E_{out} (J)	M H_2O (g)	E_{in} (J)	Faraday Efficiency (%)	Apparent Excess Heat (%)	E_{ex}/E_{in} (%)
0.350	---	2.8312	257013	157848	6.27	156945	78.92	21.22	0.58
0.350	---	0.9778	88354	54063	2.11	54678	76.90	21.32	−1.13
0.350	---	1.0531	94248	57928	2.30	57540	77.83	23.03	0.67
0.350	---	0.1867	16720	10113	0.39	10495	74.45	20.97	−3.65
0.350	---	0.7348	65533	40109	1.63	39518	79.05	22.95	1.49
0.350	---	1.0519	93092	56998	2.30	56384	77.92	23.96	1.09
0.350	---	3.0014	268014	165881	6.50	164275	77.18	24.17	0.98
0.350	---	0.9837	88652	54189	2.15	54338	77.88	21.51	−0.28
0.350	---	1.0074	89695	55164	2.18	54902	77.11	23.75	0.48
0.350	---	1.2000	107201	65842	2.64	65067	78.40	23.17	1.19
0.179	---	0.7867	33692	21470	0.81	20764	71.74	36.99	3.40
0.179	---	4.0502	171057	106821	3.99	107377	68.64	36.44	−0.52
0.179	---	0.9763	41346	26163	0.92	26663	65.66	37.82	−1.88
0.600	---	0.9097	146848	94372	3.39	92744	77.47	22.55	1.75
0.600	---	0.7971	129553	82505	3.00	81673	78.24	20.70	1.02

[a]This cell had no additives.

Cells W15E5 and W17E4 (the noncontaminated cells) operated as closed cells for 15 days at a current of 0.35 A. None of the cells showed any excess heat.

Because of the high level of interest in heavy water experiments involving the original Fleischmann and Pons configuration, i.e., palladium cathodes in LiOD and D_2O electrolytes, a large number of experiments were performed in such cells as well using a large variety of metallurgically different palladium. Twenty eight closed cells and 126 open cells were operated for a total of 1440 and 2760 cell-days, respectively. The heavy water cells were operated at much higher current densities than the light water cells, so the Faraday efficiency should be higher. However, since none of these cells showed any excess heat, no attempts were made to measure the Faraday efficiency. A detailed description of the heavy water experiments would belong in a separate publication.

TABLE V

Excess Heat—Overall Weighted Average

Cell Number	E_{ex}/E_{in} (%)
W12E6	−1.17 ± 2.15
W15E5	−1.65 ± 1.39
W16E7	0.35 ± 0.75
W17E4	0.58 ± 0.74
Grand total	0.13 ± 0.48

VII. CONCLUSIONS

Some of the most critical questions regarding reported observations of excess heat in light water cells have been answered by this research. We have clearly demonstrated that the Faraday efficiency may not be taken for granted. Internal recombination of hydrogen and oxygen is most likely to be the primary mechanism for reduced Faraday efficiency; however, other mechanisms, like parasitic electrochemical reactions not involving generation of hydrogen or oxygen, may also be present.

In the area of calorimetry, we have demonstrated that an absolute accuracy of better than 0.03% of integrated input power can be obtained and maintained for many months, provided that construction and calibration of the calorimeter is performed rigorously.

Even though this research was not intended to test the validity of the Mills and Kneizys theory, the results obtained lead to a clear conclusion as to whether or not the postulated "hydrino" atoms or molecules were formed. If "dihydrino molecules that do not combine with oxygen" were to be formed as postulated by this theory, the gas monitor should have detected an anomalous increase in the overall gas volume of the cell/recombination-vessel system. The lack of any volume

increase beyond the reported 0.6% of recombiner inefficiency, combined with the fact that the overall energy input and output are balanced to within better than 0.5%, preclude formation of any such novel atoms or molecules in these cells.

The application of highly accurate and rigorous calorimetry as presented in this research combined with proper accounting for the actual Faraday efficiency clearly indicate that the apparent excess heat observed in these experiments is a result of neglected conventional chemistry. This conclusion is supported by the lack of any excess heat in the closed cells as well.

Finally, in the heavy water arena, we have performed many experiments involving the original Pd-D_2O Fleischmann and Pons configuration. None of these experiments revealed the presence of excess heat, so no conclusions could be drawn regarding a reduced Faraday efficiency as a possible source of apparent excess heat in heavy water cells. Therefore, the following question still remains open: Are the conditions that give rise to apparent excess heat in heavy water cells the same conditions that cause an equivalent reduction in the Faraday efficiency? To find out whether excess heat in heavy water cells can also be explained by simple chemistry, all reports claiming the observation of excess heat should be accompanied by simultaneous measurements of the actual Faraday efficiency.

ACKNOWLEDGMENTS

The authors would like to thank A. G. Bose for supporting this research; D. Thomas, W. R. Short, and F. Bistany for assistance in setting up the laboratory facility; E. F. Mallove for inspiring the research in this field and for many fruitful discussions; and P. Hagelstein and M. C. H. McKubre for reviewing the manuscript.

REFERENCES

1. R. L. MILLS and S. P. KNEIZYS, "Excess Heat Production by the Electrolysis of an Aqueous Potassium Carbonate Electrolyte and the Implications for Cold Fusion," *Fusion Technol.*, **20**, 65 (1991).

2. V. C. NONINSKI, "Excess Heat During the Electrolysis of a Light Water Solution of K_2CO_3 with a Nickel Cathode," *Fusion Technol.*, **21**, 163 (1992).

3. R. T. BUSH, "A Light Water Excess Heat Reaction Suggests That 'Cold Fusion' May Be 'Alkali-Hydrogen' Fusion," *Fusion Technol.*, **22**, 301 (1992).

4. R. NOTOYA, "Cold Fusion by Electrolysis in a Light Water–Potassium Carbonate Solution with a Nickel Electrode," *Fusion Technol.*, **24**, 202 (1993).

5. M. SRINIVASAN et al., "Tritium and Excess Heat Generation During Electrolysis of Aqueous Solutions of Alkali Salts with Nickel Cathode," Frontiers of Cold Fusion, *Proc. 3rd Conf. Cold Fusion*, Nagoya, Japan, October 21–25, 1992, p. 123.

6. M. FLEISCHMANN and S. PONS, "Electrochemically Induced Nuclear Fusion of Deuterium," *J. Electroanal. Chem.*, **261**, 301 (1989).

7. M. FLEISCHMANN and S. PONS, "Calorimetry of the Pd-D_2O System: From Simplicity via Complications to Simplicity," *Phys. Lett. A*, **176**, 118 (1993).

8. R. D. EAGLETON and R. T. BUSH, "Calorimetric Experiments Supporting the Transmission Resonance Model for Cold Fusion," *Fusion Technol.*, **20**, 239 (1991).

9. M. C. H. McKUBRE et al. "Calorimetry and Electrochemistry in the D/Pd System," *Proc. 1st Annual Conf. Cold Fusion*, Salt Lake City, Utah, March 28–31, 1990, p. 20.

10. E. STORMS, "Measurements of Excess Heat from a Pons-Fleischmann-Type Electrolytic Cell Using Palladium Sheet," *Fusion Technol.*, **23**, 230 (1993).

11. *CRC Handbook of Chemistry and Physics*, 5-19, CRC Press (1992–1993).

12. M. C. H. McKUBRE, SRI International, Private Communication (1992).

13. S. I. SMEDLEY, S. CROUCH-BAKER, M. C. H. McKUBRE, and F. L. TANZELLA, "The January 2, 1992 Explosion in a Deuterium/Palladium Electrolytic System at SRI International," *Proc. 3rd Int. Conf. Cold Fusion*, Nagoya, Japan, October 21–25, 1992, p. 139.

14. R. T. BUSH, Private Communication during the 4th Int. Conf. Cold Fusion, Maui, Hawaii, December 6–9, 1993.

15. M. SRINIVASAN et al., "Excess Heat and Tritium Measurements in Ni-H_2O Electrolytic Cells," *Proc. Int. Symp. Cold Fusion and Advanced Energy Sources*, Minsk, Belarus, May 24–26, 1994.

Zvi Shkedi (PhD, physics, The Weitzmann Institute of Science, Rehovot, Israel, 1977) is a principal engineer at Bose Corporation. His interests include precision measurement technology, materials aspects of sensors and transducers, and practical applications of new technology.

Robert C. McDonald (PhD, chemistry, Boston University, 1975) was a research engineer at Bose Corporation where he focused on electrochemical cells. His interests include lithium batteries.

John J. Breen (MSME, Rochester Institute of Technology, 1984) is a research engineer at Bose Corporation.

Stephen J. Maguire (BS, electrical engineering technology, Wentworth Institute of Technology, 1994; BS, wood science and technology, University of Massachusetts, 1980) is an electrical engineering technologist at Bose Corporation. His interests include practical applications of power conversion.

Joe Veranth (MSEE, MIT, 1970) is vice president of research and development at Bose Corporation. His interests include nonlinear control systems, psychoacoustics, power processing, and total quality.